2013

Effects of membrane fouling on N-nitrosamine rejection by nanofiltration and reverse osmosis membranes

Takahiro Fujioka
University of Wollongong, tf385@uowmail.edu.au

Stuart J. Khan
University Of New South Wales, s.khan@unsw.edu.au

James A. McDonald
University Of New South Wales

Rita K. Henderson
University Of New South Wales, r.henderson@unsw.edu.au

Yvan Poussade
Veolia Water Australia, yvan.poussade@veoliawater.com.au

See next page for additional authors

Publication Details

Fujioka, T., Khan, S. J., McDonald, J. A., Henderson, R. K., Poussade, Y., Drewes, J. E. & Nghiem, L. D. (2013). Effects of membrane fouling on N-nitrosamine rejection by nanofiltration and reverse osmosis membranes. Journal of Membrane Science, 427 311-319.

Effects of membrane fouling on N-nitrosamine rejection by nanofiltration and reverse osmosis membranes

Revised version submitted to

Journal of Membrane Science

September 2012

Takahiro Fujioka [1], Stuart J. Khan [2], James A. McDonald [2], Rita K. Henderson [2], Yvan Poussade [3,4], Jörg E. Drewes [2, 5], and Long D. Nghiem [1,*]

[1] Strategic Water Infrastructure Laboratory, School of Civil Mining and Environmental Engineering, The University of Wollongong, NSW 2522, Australia

[2] UNSW Water Research Centre, School of Civil and Environmental Engineering, The University of New South Wales, NSW 2052, Australia

[3] Veolia Water Australia, Level 15, 127 Creek Street, QLD 4000, Australia

[4] Seqwater, Level 2, 240 Margaret St, Brisbane City QLD 4000 Australia

[5] Advanced Water Technology Center (AQWATEC), Department of Civil and Environmental Engineering, Colorado School of Mines, Golden, CO 80401, USA

* Corresponding author: Long Duc Nghiem, Email: longn@uow.edu.au, Ph +61 2 4221 4590

LIST OF FIGURES

Figure 10: N-nitrosamine rejections by the ESPA2 membrane with and without fouling of (a) SA, (b) HA, (c) BSA and (d) Ludox CL. (20 mM NaCl, 1 mM $NaHCO_3$, 1 mM $CaCl_2$, permeate flux 20 L/m^2h, cross flow velocity 40.2 cm/s, feed pH 8.0 ± 0.1, feed temperature 20.0 ± 0.1 ºC). Error bars show the standard deviation of two replicate experiments.

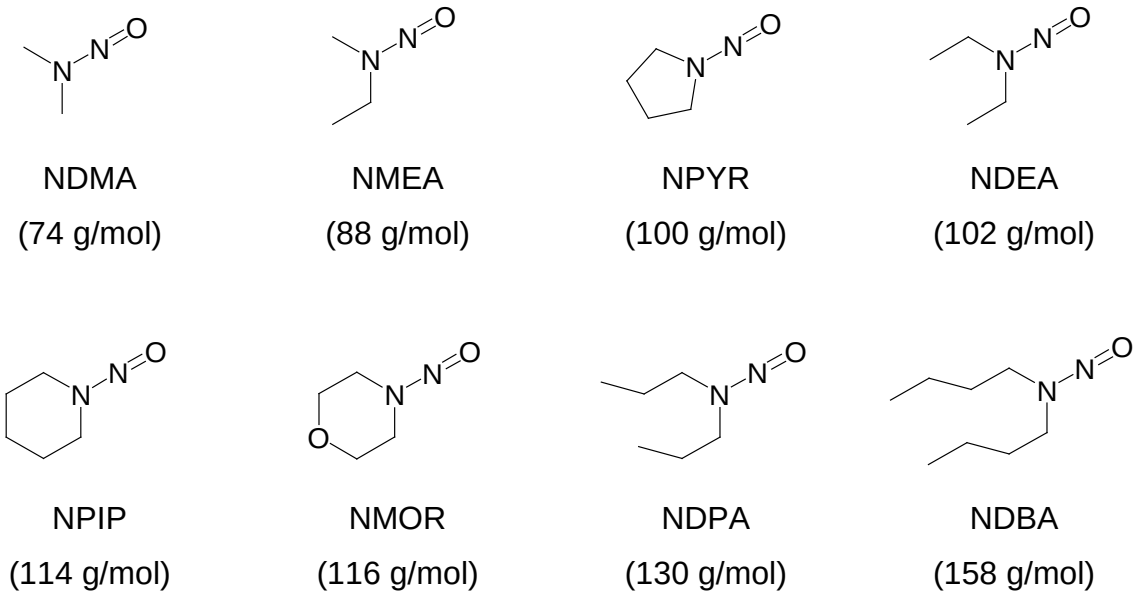
NDMA
(74 g/mol)
NMEA
(88 g/mol)
NPYR
(100 g/mol)
NDEA
(102 g/mol)
NPIP
(114 g/mol)
NMOR
(116 g/mol)
NDPA
(130 g/mol)
NDBA
(158 g/mol)

Figure 1

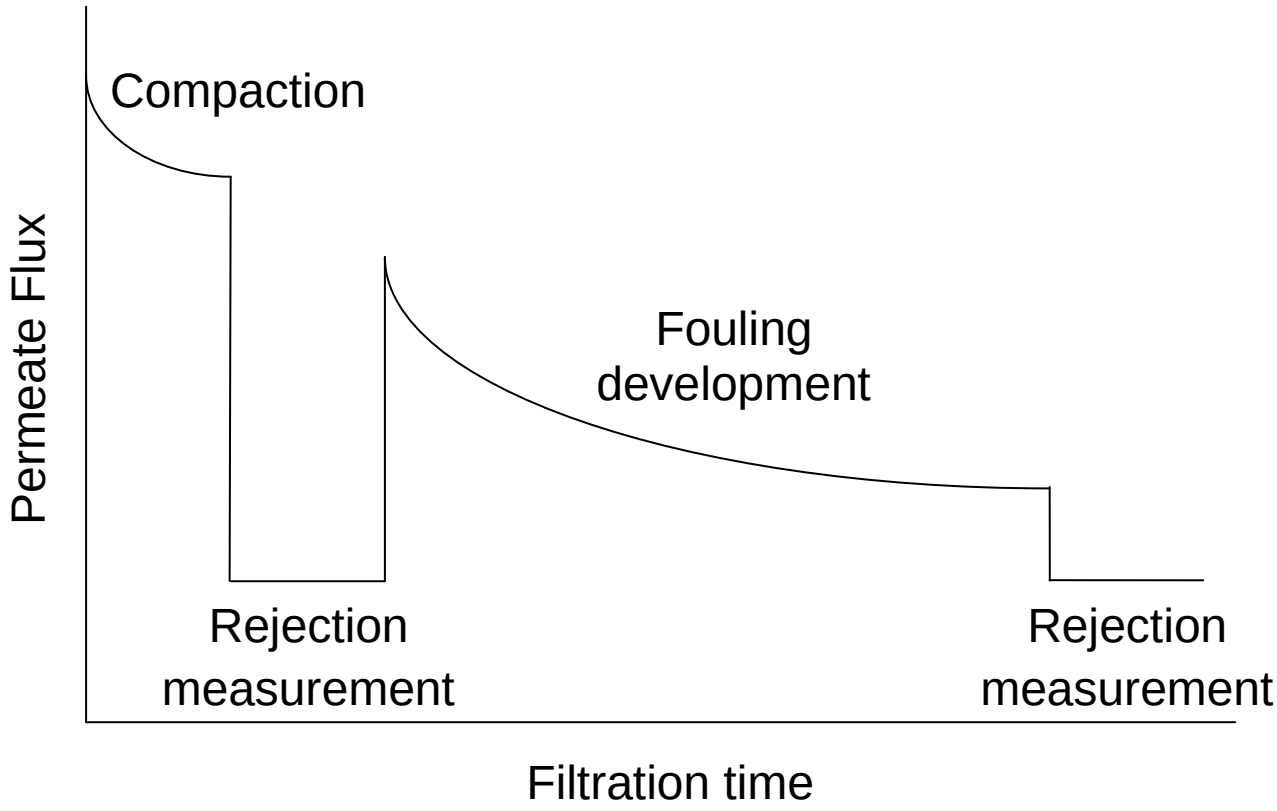
Compaction
Permeate Flux
Fouling
development
Rejection
measurement
Rejection
measurement
Filtration time

Figure 2

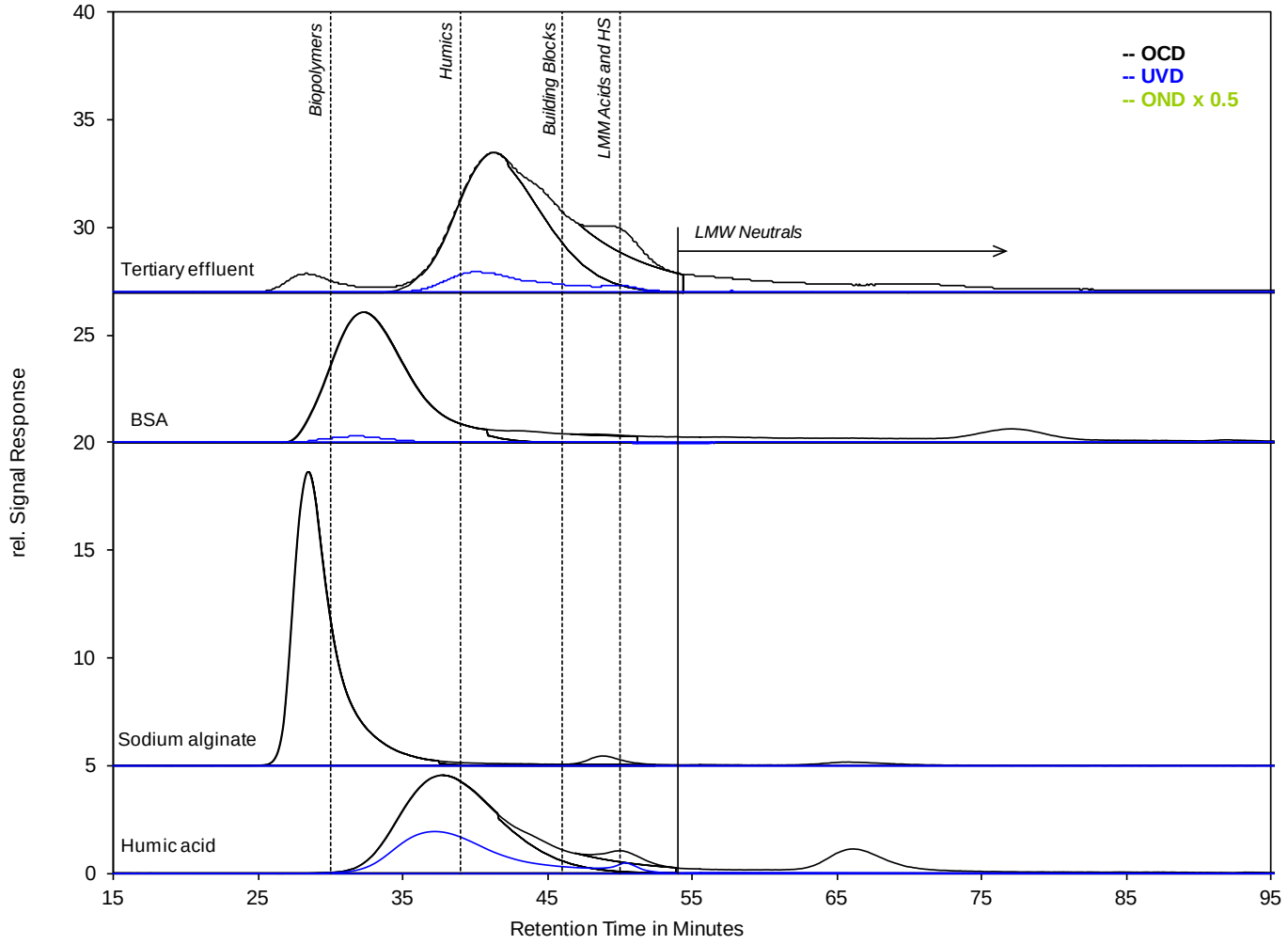
Biopolymers
Humics
Building Blocks
LMM Acids and HS
LMW Neutrals
-- OCD
-- UVD
-- OND x 0.5
Tertiary effluent
BSA
Sodium alginate
Humic acid
rel. Signal Response
Retention Time in Minutes
40
35
30
25
20
15
10
5
0
15
25
35
45
55
65
75
85
95

Figure 3

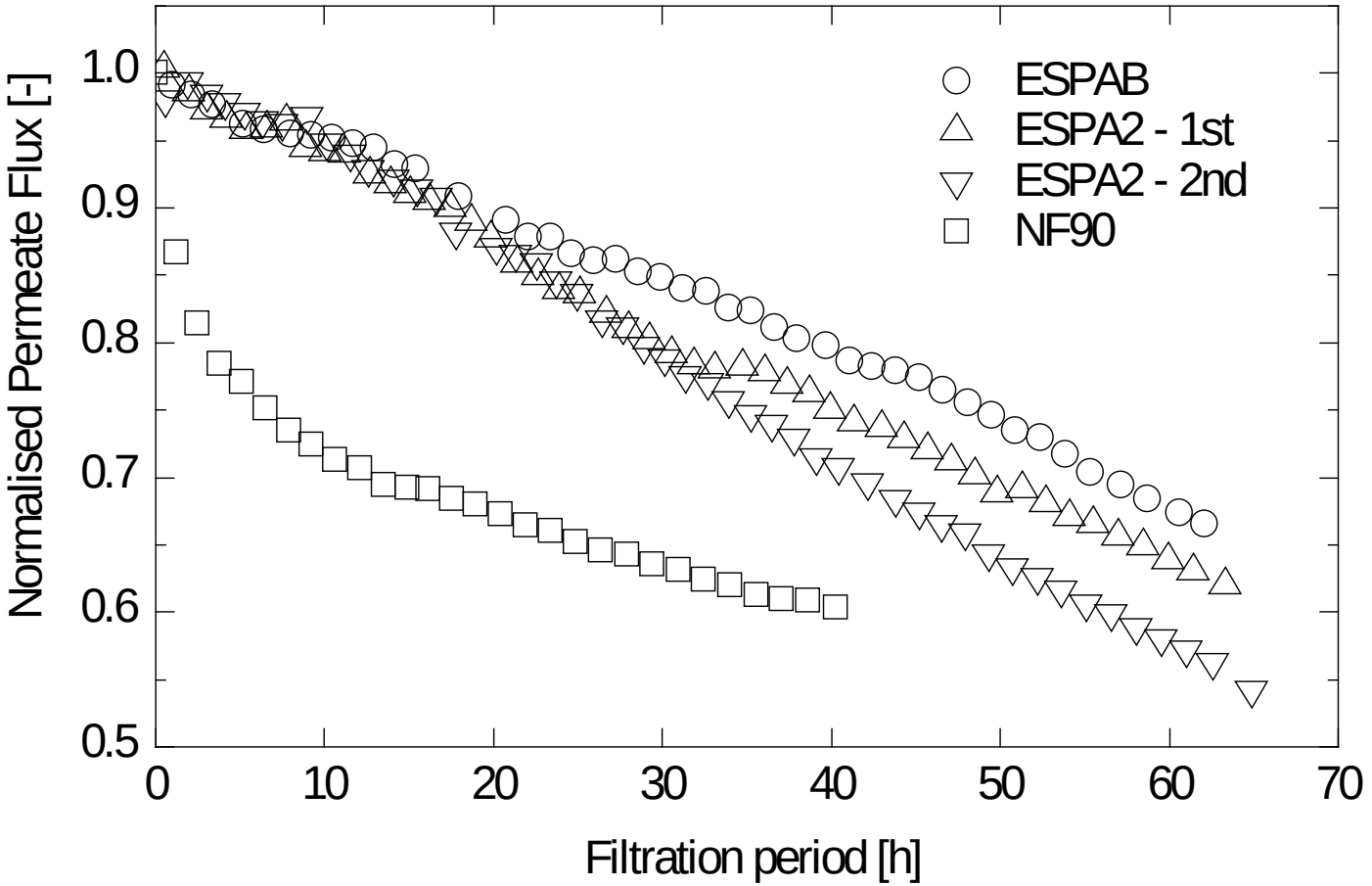
Normalised Permeate Flux [-]
1.0
0.9
0.8
0.7
0.6
0.5
0
10
20
30
40
50
60
70
Filtration period [h]
ESPAB
ESPA2 - 1st
ESPA2 - 2nd
NF90

Figure 4

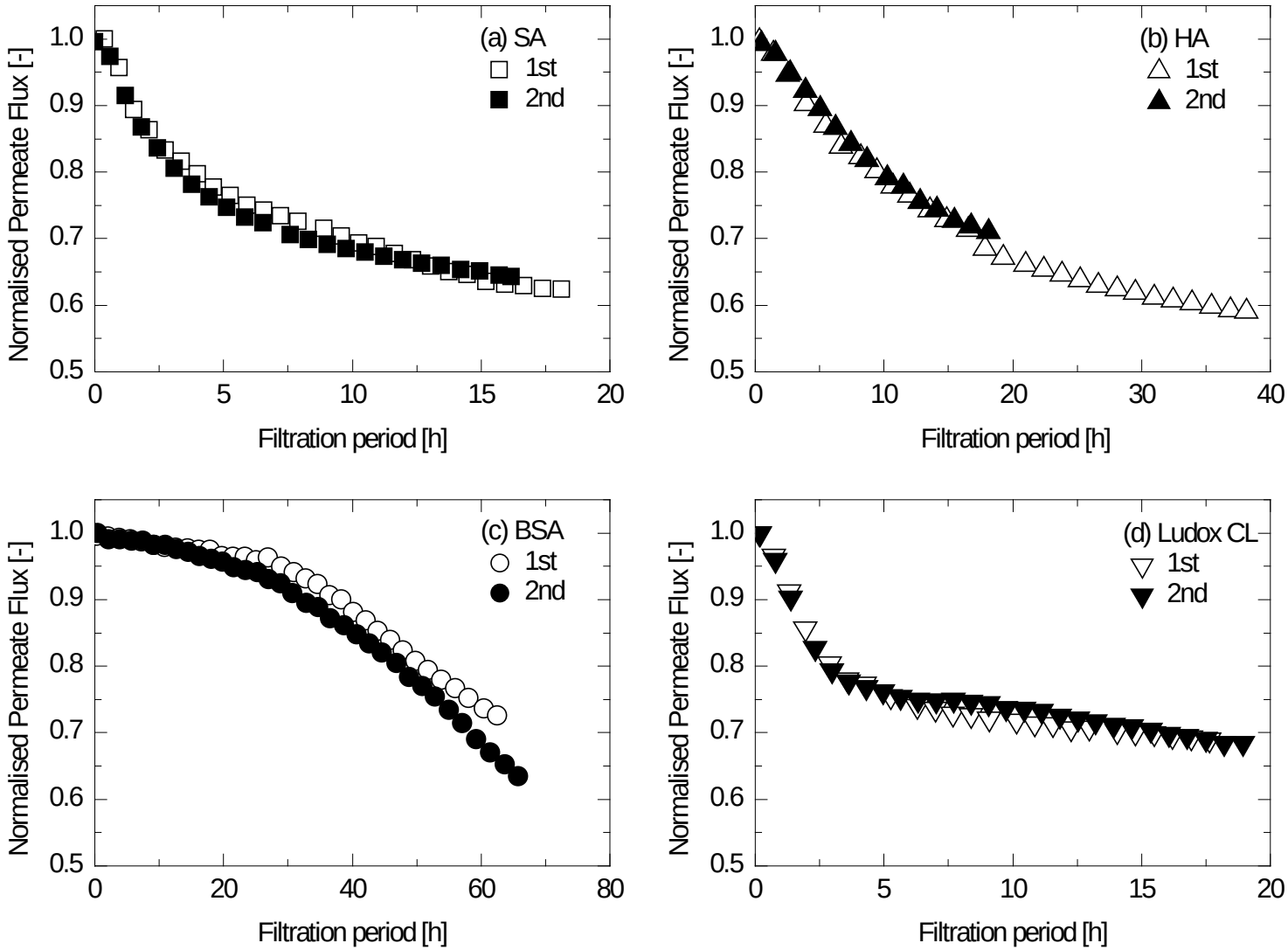
(a) SA
1st
2nd
(b) HA
1st
2nd
(c) BSA
1st
2nd
(d) Ludox CL
1st
2nd
Normalised Permeate Flux [-]
Filtration period [h]
1.0
0.9
0.8
0.7
0.6
0.5
0
5
10
15
20
30
40
60
80

Figure 5

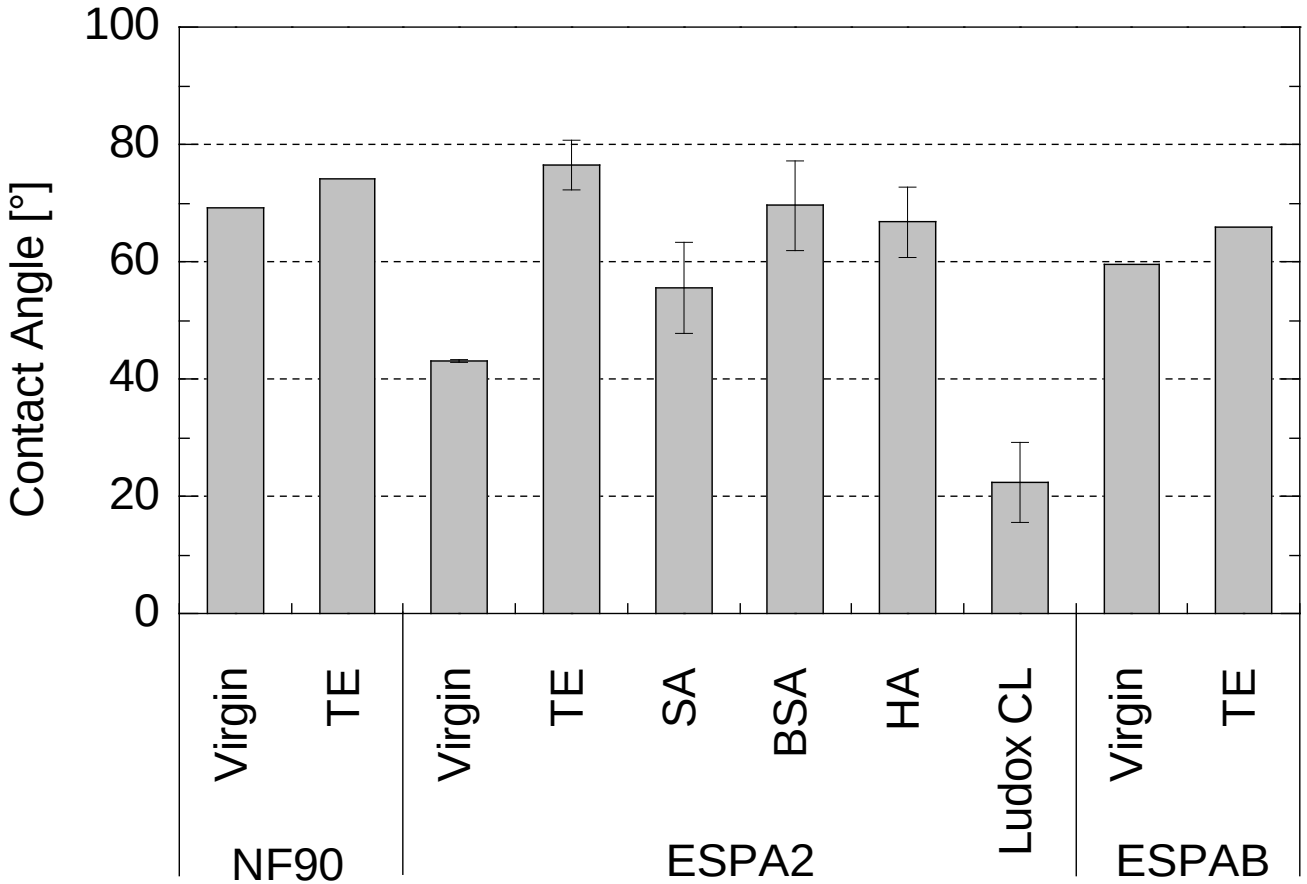
Contact Angle [°]
100
80
60
40
20
0
Virgin
TE
Virgin
TE
SA
BSA
HA
Ludox CL
Virgin
TE
NF90
ESPA2
ESPAB

Figure 6

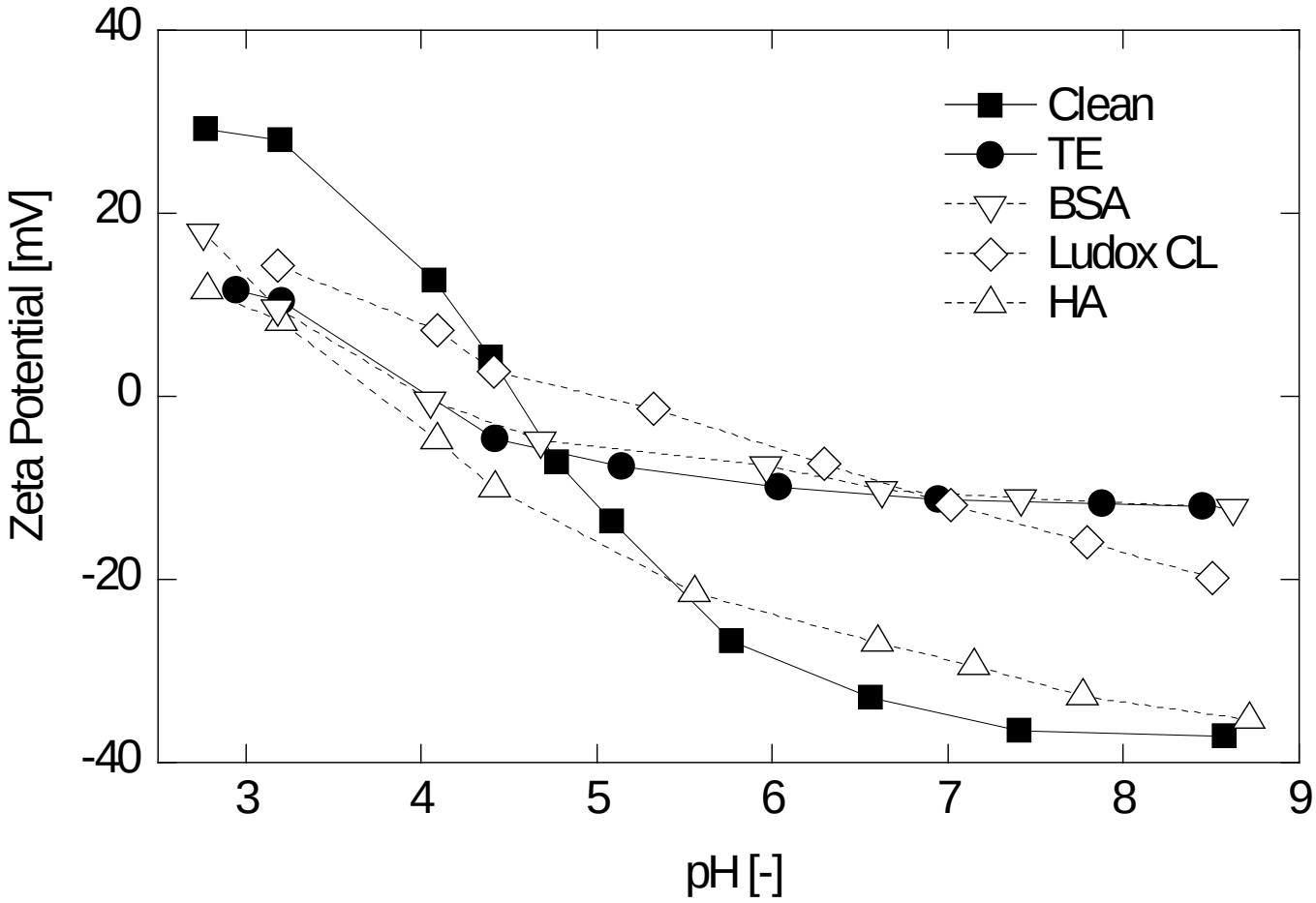
40
20
0
-20
-40
Zeta Potential [mV]
3
4
5
6
7
8
9
pH [-]
Clean
TE
BSA
Ludox CL
HA

Figure 7

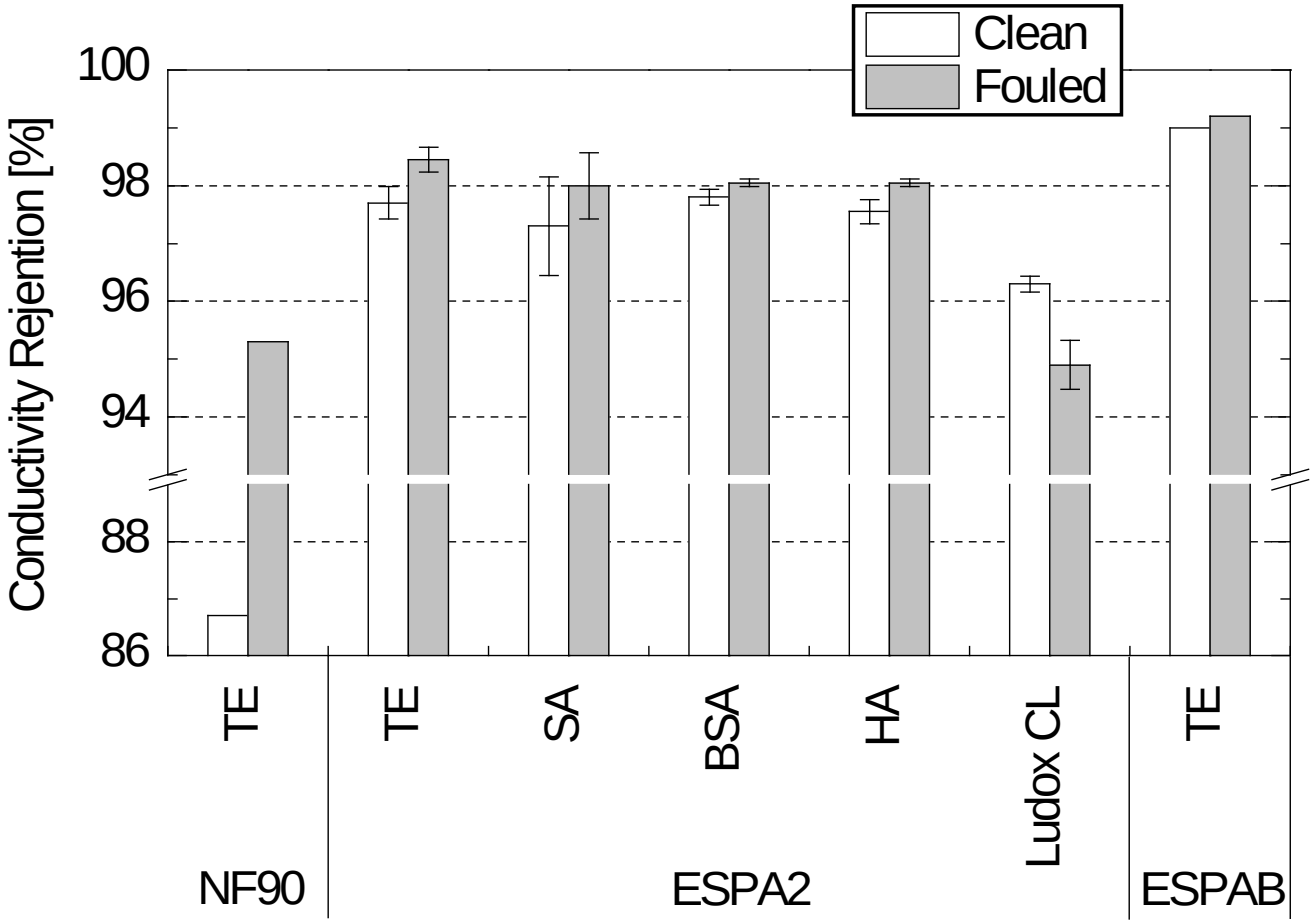
Clean
Fouled
Conductivity Rejention [%]
100
98
96
94
88
86
TE
TE
SA
BSA
HA
Ludox CL
TE
NF90
ESPA2
ESPAB

Figure 8

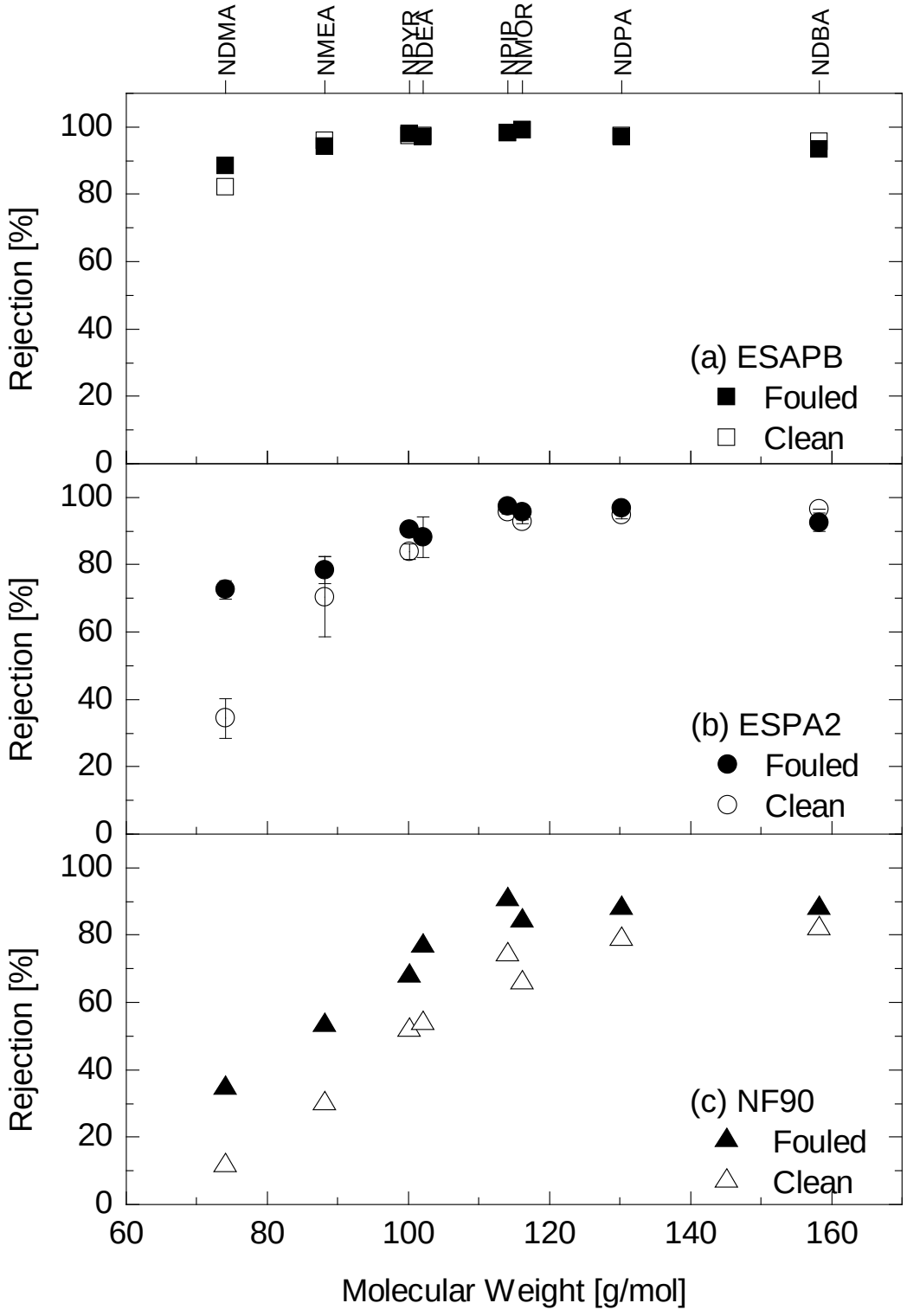

1031

1032 **Figure 9**

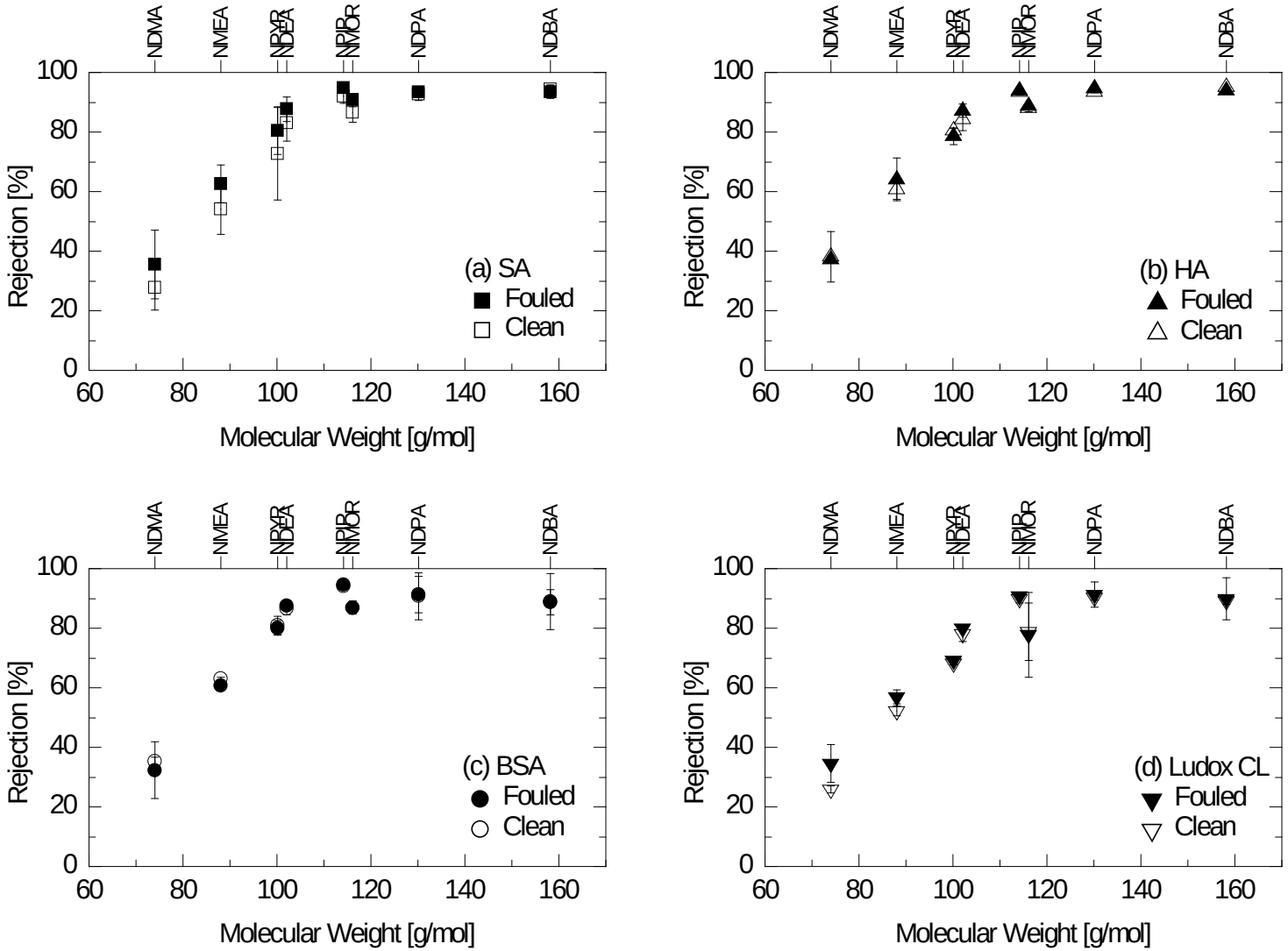
NDMA
NMEA
NPYR
NDEA
NPIP
NMOR
NDPA
NDBA
Rejection [%]
Molecular Weight [g/mol]
(a) SA
Fouled
Clean
(b) HA
Fouled
Clean
(c) BSA
Fouled
Clean
(d) Ludox CL
Fouled
Clean

Figure 10

Abstract

The impact of fouling on N-nitrosamine rejection by nanofiltration (NF) and reverse osmosis (RO) membranes was investigated in this study. Membrane fouling was simulated using tertiary treated effluent and several model fouling solutions (that contained sodium alginate, bovine serum albumin, humic acid or colloidal silica) to elucidate the changes in rejection behaviour of N-nitrosamines. In general, the rejection of N-nitrosamines increased when the membranes were fouled by tertiary effluent. The rejection of small molecular weight N-nitrosamines was most affected by membrane fouling. In particular, the rejection of N-nitrosodimethylamine (NDMA) by the ESPA2 membrane increased from 34 to 73% after membrane fouling caused by tertiary effluent. The results also indicate that the impact was less apparent for the lowest permeability membrane (i.e., ESPAB), and the rejection of N-nitrosamines by the ESPAB membrane was over 82% regardless of membrane fouling. The effect of membrane fouling caused by model foulants on N-nitrosamine rejection was considerably less than that caused by tertiary effluent. Size exclusion chromatography analyses revealed that the tertiary effluent contains a high fraction of low molecular weight (< 500 g/mol) organic substances. It appears that these low molecular weight foulants present in the tertiary effluent can restrict the solute pathway within the active skin layer of membranes, resulting in the observed increase of solute rejection.

Keywords: Water recycling, N-nitrosamines, NDMA, reverse osmosis, organic fouling, colloidal fouling.

1. Introduction

Augmentation of potable water sources with reclaimed municipal effluent is an important strategy to secure a reliable water supply in regions and countries with severe water scarcity. However, a major concern over this alternative source of water supply is the occurrence of trace organic chemicals which may induce adverse and chronic health effects. Notable amongst these trace organic chemicals is N-nitrosodimethylamine (NDMA) which is an N-nitrosamine that can be formed during the chloramination of the treated effluent [1]. In addition to NDMA, other N-nitrosamines known to occur in treated effluent include N-nitrosomethylethylamine (NMEA), N-nitrosopyrrolidine (NPYR), N-nitrosodiethylamine (NDEA), N-nitrosopiperidine (NPIP), N-nitrosomorpholine (NMOR), N-nitrosodipropylamine (NDPA), N-nitrosodi-n-butylamine (NDBA) [2-4]. Some of these N-nitrosamines have been identified as probable carcinogenic agents and thus their concentrations in drinking water and recycled water intended for potable consumption have been regulated by water authorities around the world [5-6]. The Australian Guidelines for Water Recycling have recommended the maximum value of NDMA, NDEA, and NMOR in recycled water intended for potable supply of 10, 10, and 1 ng/L, respectively [7]. Both reverse osmosis (RO) and nanofiltration (NF) membranes have been frequently used in water reclamation partly to ensure adequate removal of emerging trace chemicals, little is known about their capacity to remove N-nitrosamines in full-scale installations. Reported percentage rejections of NDMA vary greatly in full-scale plants from almost negligible to 86% and the underlying reason for such significant variation in NDMA rejection remains unclear [8-11].

To date, only a few laboratory-scale studies have investigated N-nitrosamine rejection capability of NF/RO membranes using clean matrix solutions [3, 12-13]. These studies reported that the rejection of NDMA by RO membranes was in the range from 50 to 70%. The rejection of N-nitrosamines increased in the order of increasing molecular weight and the steric hindrance mechanism was identified as a predominant rejection mechanism of N-nitrosamines by NF/RO membranes [3, 12-13]. Feed solution characteristics (i.e., pH, ionic strength and temperature of the feed solution) also affected the rejection of NDMA and in some cases other N-nitrosamines [3, 13]. In particular, Fujioka et al. [13] reported a significant drop in NDMA rejection (from 49 to 25%) for an increase in feed temperature from 20 to 30 ºC. Nevertheless, the variations in these feed solution characteristics explain

only some of the variations in NDMA rejections that were reported in the previous full-scale studies.

Municipal wastewater usually contains a large amount of organic and inorganic matter, resulting in the formation of organic and colloidal fouling, bio-fouling and inorganic scales on RO membranes [14-15]. It has been established in the literature that membrane fouling can either increase or decrease the separation efficiency of NF/RO membranes [14, 16-18]. However, apart from a laboratory-scale study conducted by Steinle-Darling et al. [3] who investigated the rejection of several N-nitrosamines by an RO membrane (ESPA3) artificially fouled with sodium alginate, to date little attention has been given to the effects of membrane fouling on the rejection of N-nitrosamines. Steinle-Darling et al. [3] reported that membrane fouling by sodium alginate on the ESPA3 membrane caused a reduction in NDMA rejection (from 56 to 37%).

The aim of this work was to provide insights into the effects of membrane fouling on the rejection of N-nitrosamines by NF/RO membranes. The effects of membrane fouling were investigated by comparing the rejections of N-nitrosamines by clean and fouled membranes. Tertiary treated effluent and four different model foulants (namely sodium alginate, bovine serum albumin, humic acid and colloidal silica) were used to induce membrane fouling. The tertiary treated effluent and model foulants were characterised in detail to systematically elucidate the effects of membrane fouling on the rejection of N-nitrosamines by NF/RO membranes.

2. Materials and methods

2.1. NF/RO membranes

Three NF/RO membranes – namely the NF90, ESPA2, and ESPAB – were used in this investigation. These are thin-film composite polyamide membranes with a microporous supporting layer and were supplied as flat sheet samples. Key properties of these membranes are shown in Table 1. The NF90 (Dow Filmtec, Minneapolis, MN, USA) is an NF membrane typically used for softening of brackish water. The ESPA2 (Hydranautics, Oceanside, CA, USA) is a low pressure reverse osmosis membrane that is widely applied for water reclamation applications. The ESPAB (Hydranautics, Oceanside, CA, USA) is also low pressure reverse osmosis but it has been designed to achieve a high boron rejection.

[Table 1]

2.2. Chemicals

The eight N-nitrosamines used in this study (Figure 1) were of analytical grade and were purchased from Sigma-Aldrich (St Louis, MO, USA). Their physicochemical properties have been described in detail elsewhere [13]. N-nitrosamine stock solution was prepared in pure methanol with 250 µg/L of each N-nitrosamine. A deuterated surrogate standard was used for each N-nitrosamine under investigation. These surrogate standards include N-nitrosodimethylamine-D6, N-nitrosomethylethylamine-D3, N-nitrosopyrrolidine-D8, N-nitrosodiethylamine-D10, N-nitrosopiperidine-D10, N-nitrosomorpholine-D8, N-nitrosodipropylamine-D14 and N-nitrosodi-n-butylamine-D9, and were purchased from CDN isotopes (Pointe-Claire, Quebec, Canada). A surrogate stock solution containing 100 µg/L of each deuterated N-nitrosamine was prepared in pure methanol. The stock solutions were stored at -18 ºC and used within one month of preparation.

Analytical grade NaCl, $CaCl_2$ and $NaHCO_3$ were purchased from Ajax Finechem (Taren Point, NSW, Australia). Sodium alginate (SA), bovine serum albumin (BSA), humic acid (HA) and colloidal silica (Ludox CL, 30% weight suspension in water) were selected as model foulants to simulate polysaccharides, proteins, refractory organic matter and colloidal particles, respectively. These model foulants were purchased from Sigma-Aldrich (St Louis, MO, USA). The Ludox CL is a positively charged silica particle whose surface is coated with a layer of aluminium [19]. The hydrodynamic diameter of the Ludox CL is from approximately 40 nm at below pH 6 to 233 nm at pH 10 due to aggregation effects in different pH solutions [19].

[Figure1]

2.3. Tertiary treated effluent

Tertiary treated effluent sample was collected from an advanced water recycling plant in New South Wales, Australia. The treatment train of the plant prior to the sampling point includes screening, bioreactor and sand filtration, and the sample was collected after sand filtration.

2.4. Membrane filtration system

A laboratory-scale cross flow NF/RO filtration system was used in this study (Supplementary Material Figure S1). A detailed description of this system is available elsewhere [13]. The system consisted of a cross-flow stainless steel cell with effective membrane area of 4 cm by 10 cm and a channel height of 2 mm. The feed solution was kept in a stainless reservoir and was fed to the membrane cell by a high pressure pump (Hydra-Cell, Wanner Engineering Inc., Minneapolis, MN, USA). The permeate flow and cross-flow velocity were regulated by a bypass valve and a back-pressure regulator (Swagelok, Solon, OH, USA). The permeate flow was monitored using a digital flow meter (FlowCal, GJC Instruments Ltd, Cheshire, UK) which was connected to a computer. A stainless steel heat exchanging coil was submerged into the feed reservoir and was connected to a chillier/heater unit (Neslab RTE 7, Thermo Scientific Inc., Waltham, MA, USA) to control the temperature of the feed solution.

2.5. Experimental protocols

Rejection measurement and membrane fouling development were sequentially carried out with four steps: (1) compaction; (2) measuring N-nitrosamine rejection without membrane fouling; (3) fouling development; and (4) remeasuring N-nitrosamine rejection by fouled membrane (Figure 2). Because full-scale RO plants are generally operated with a constant (average) permeate flux which is approximately 20 L/m^2h [20] and feed pressure increases as fouling progresses to maintain the permeate flux, the constant permeate flux of 20 L/m^2h was used to evaluate N-nitrosamine rejection before and after fouling. Throughout the experiments, cross flow velocity and feed temperature in the reservoir were always kept constant at 0.42 m/s and 20 ± 0.1 ºC, respectively. The details of these four steps are as follows.

Step 1: The membrane sample was first compacted using Milli-Q water at 1,800 kPa until the permeate flux was stabilised.

Step 2: Following the compaction step, the Milli-Q water in the filtration system was replaced with either the tertiary effluent or synthetic solution containing a particular model foulant (e.g. SA, HA, BSA or Ludox CL) and background electrolytes (20 mM NaCl, 1 mM $CaCl_2$ and 1 mM $NaHCO_3$). The concentrations of SA, BSA and HA in the feed solution were adjusted to make up approximately 10 mg/L as total organic carbon (TOC). The Ludox

CL was suspended in the same background electrolyte solution (20 mM NaCl, 1 mM $CaCl_2$ and 1 mM $NaHCO_3$) to obtain 100 mg/L of colloidal silica. After the replacement of feed solutions, stock N-nitrosamine solution was spiked into the feed solution at environmentally relevant concentration (i.e., 250 ng/L). The permeate flux was also adjusted at 20 L/m^{2}h which is a typical value for most water reclamation RO plants [20]. The system was operated for 1 h prior to the collection of the feed and permeate samples for analysis. This sampling point represents the performance of the membrane under a clean condition.

Step 3: After the first sampling event, membrane fouling was promoted by adjusting the permeate flux to 60 L/m^{2}h. The system was then continuously operated with a constant feed pressure. The fouling development step ended after the permeate flux reached 45 L/m^{2}h (i.e., decreased by 25%).

Step 4: The permeate flux was adjusted to 20 L/m^{2}h and the system was stabilised for 1 h prior to the second sampling of the feed and permeate. This sampling point represents the performance of the membrane under a fouled condition.

[Figure 2]

2.6. Analytical techniques

2.6.1. Size exclusion chromatography analyses

Characterisation of dissolved organic carbon (DOC) composition in the tertiary effluent and model foulant solution samples was carried out with a size exclusion chromatography technique using a Liquid Chromatography - Organic Carbon Detection (LC-OCD) Model 8 system (DOC-LABOR, Karlsruhe, Germany). The LC-OCD system is equipped with a UV-detector (254 nm) as well as organic carbon and nitrogen detectors. Chromatographic separation is undertaken using a Toyopearl® TSK HW-50S column (Tosoh Bioscience, Tokyo, Japan). Prior to the analysis, calibration of humic substance molecular weights was conducted using IHSS Humic acid and IHSS Fulvic acid. Calibrations of detectors for total organic carbon and total organic nitrogen were also conducted using potassium hydrogen phthalate and potassium nitrate, respectively. For the analysis, a mobile phase (phosphate buffer, pH 6.37, 2.5 g/L KH_2PO_4 and 1.5g/L $Na_2HPO_4 \cdot H_2O$) was set at a flow rate of 1.1 mL/min. In the LC-OCD system, an injected sample of 1 mL was pre-filtered with an in-line

0.45 µm PES-filter located in front of the column and detectors. Software provided by the manufacturer (ChromCALC, DOC-LABOR, Karlsruhe, Germany) was used for the quantification of the organic matter compositions. Further details can also be found in previous studies [21-22].

2.6.2. Contact angle measurement

Contact angle of membrane surface was measured using the standard sessile drop method. This was performed with a Rame-Hart Goniometer (Model 250, Rame-Hart, Netcong, NJ). Prior to the measurement, virgin and fouled membrane samples were dried for over 24 h in the dark. The dry membrane was fixed on the stage of the instrument and contact angle of the membrane was measured with a water droplet (Milli-Q water). The contact angle of each membrane was determined with an average of ten droplets.

2.6.3. Zeta potential measurement

Zeta potential of the virgin and fouled membrane surface was determined and calculated using the Fairbrother-Mastin streaming potential method. The measurement of the streaming potential was performed between pH 3 and 8.5 with a SurPASS Electrokinetic Analyser (Anton Paar GmbH, Graz, Austria). In the measurement, 1 mM KCl was used as a background electrolyte solution. The background solution pH was adjusted by a titration of either KOH (1M) or HCl (1M) solutions. During the analysis, the background solution temperature was 25±1°C.

2.6.4. Basic analytical techniques

Turbidity was analysed using a 2100N laboratory turbidity meter (Hach, USA). Conductivity and pH were measured using an Orion 4-Star Plus pH/conductivity meter (Thermo scientific, USA). TOC concentration was determined using a TOC-VSH analyser (Shimadzu, Japan) based on the non-purgeable organic carbon (NPOC) method. Cations and anions were analysed using an Inductive Coupled Plasma – Mass Spectrometer (7500CS, Agilent Technologies, Wilmington, DE, USA) and an ion chromatography (IC) system (Shimadzu, Tokyo, Japan), respectively.

196 2.6.5. N-nitrosamine concentration analysis

197 The analysis of each N-nitrosamine concentration in this study is based on the gas
198 chromatography coupled with tandem mass spectrometry (GC-MS/MS) technique using
199 electron ionisation in a combination with the solid phase extraction (SPE) method previously
200 described by McDonald et al [23]. Prior to the SPE process, the SPE cartridges
201 (Supelclean^{TM} Coconut Charcoal SPE cartridges (2 g/mL), Supelco, St Louis, MO, USA)
202 were cleaned with 6 mL dichloromethane, 6 mL methanol and 12 mL of Milli-Q water.
203 Accurate quantitation (accounting for incomplete SPE recovery) was undertaken by direct-
204 analogue isotope dilution for all nitrosamines by adding 100 µL surrogate stock solution into
205 200 mL of each sample to make up 50 ng/L of each N-nitrosamine surrogate. N-nitrosamines
206 in the samples were then extracted by SPE at a flow rate of 5 mL/min. The cartridges were
207 rinsed with 3 mL Milli-Q water and dried with high purity nitrogen gas for at least 60
208 minutes. The dried SPE cartridges were then eluted using 12 mL dichloromethane, and 100
209 µL of toluene was added in the eluent. The eluent was then concentrated to 1 mL with a
210 Turbovap LV (Caliper Life Sciences, Hopkinton, MA, USA) under a gentle nitrogen stream.
211 The concentrations of N-nitrosamines were quantified using an Agilent 7890A gas
212 chromatograph (GC) coupled with an Agilent 7000B triple quadrupole mass spectrometer
213 (MS/MS). Calibration curves were established for each N-nitrosamine in the range of 1-400
214 ng/L. The NMOR calibration curve was extended to account for the NMOR concentration of
215 over 400 ng/L. The quantitative detection limits of this technique for NDMA, NDEA and
216 NDPA were 5 ng/L. The quantitative detection limits for all other N-nitrosamines used in this
217 study were 10 ng/L.

218 # 3. Results and discussion

219 ## *3.1. Characteristics of the tertiary effluent and model foulants*

220 Ionic composition and organic content of the tertiary effluent used in this study (Table 3) was
221 similar to that of most water reclamation plants. Nevertheless, the conductivity of this tertiary
222 treated effluent (Table 2) was slightly lower than the typical range of 1200-1700 µS/cm,
223 which is often found in the literature [24-25]. The tertiary effluent used in this study had not
224 been subjected to chloramination, with the exception of NMOR, and all other N-nitrosamines
225 were not detectable in the tertiary effluent sample. The concentration of NMOR in this
226 tertiary effluent was 1350 ng/L. NMOR can be found in toiletry and cosmetic products [26]

and rubber and tire industry, elevated concentration of NMOR in treated effluent has previously been reported [27]. The water recycling plant where the tertiary treated effluent was collected is known to have a very high load of industrial wastewaters in its catchment.

[Table 2]

The organic contents of secondary effluents have been generally characterised to comprise a number of size fractions commonly referred to as biopolymers (polysaccharides, proteins and colloidal organics) (>>20,000 Da), humic substances (approximately 1000 Da), building blocks (300-500 Da) and low molecular weight (LMW) acids (<350 Da) and neutrals (<350 Da) [21-22, 28-29]. The building blocks block fraction represents breakdown products, or intermediates during the degradation, of humic substances such as fulvic acid [22, 30]. The tertiary effluent used in this study has a diverse molecular weight distribution (Figure 3). The DOC concentration of fractions of biopolymers (10%), humic substances (46%), building blocks (17%) and LMW neutrals (23%) in the tertiary effluent (Table 3) was in good agreement with a previous study carried out by Henderson et al. [28]. Model foulants used in this investigation had significant differences in their physicochemical characteristics which were expected to assist in identifying the impact of fouling on membrane separation performance. The major fraction of SA and BSA solutions was biopolymers (>20000 g/mol), which is consistent with a previous study [31] showing a molecular weight of 12000-80000 g/mol (SA) and 67000 g/mol (BSA). The molecular weight of HA analysed here was in the range of approximately 1000 g/mol and this is in good agreement of the average molecular weight of HA (1000 g/mol) reported in the literature [22]. All three organic model foulant also contained some fraction of building blocks (300-500 g/mol) and LMW neutrals (<350 g/mol) (Table 3).

[Figure 3]

[Table 3]

3.2. Membrane fouling behaviour

Significant membrane fouling was observed with all three membranes investigated in this study when tertiary effluent was used at the elevated initial permeate flux of 60 L/m^{2}h (which is approximately three times the value used in most full scale RO systems for water recycling

applications). The profile of membrane permeability measured before and after fouling is presented in Table S2 of the Supplementary Material. Membrane fouling behaviour of the NF90 differs significantly from that of the ESPA2 and ESPAB membranes (Figure 4). Flux decline was most severe for the NF90 membrane followed by the ESPA2 and ESPAB membranes. The permeate flux of the NF90 membrane dropped by 30% within the first 12 h system operation, and then decreased linearly as filtration progressed. In contrast, the two RO membranes (ESPAB and ESPA2) showed an almost linear flux decline from the beginning of the filtration. The flux decline of the ESPA2 and ESPAB membranes using tertiary effluent reached 30% with 40-50 h and 60 h filtration, respectively. Interestingly, the rate of flux decline amongst the three membranes increased in the order of increasing pure water membrane permeability (Table 1). Similar observations were reported in previous laboratory-scale studies [16, 32].

[Figure 4]

When the model foulants were used, significant variation in membrane fouling was observed. When the ESPA2 membrane was fouled with either SA or HA, permeate flux dropped rapidly within 10–20 h of system operation (Figure 5a-b). These observed curves of membrane fouling are consistent with a previous study [33]. The rapid flux decline in the early stage may have resulted from the formation of an alginate and humic acid fouling layer on the membrane surface, resulting in a substantial resistance to permeate flow [16, 34]. In fact, it is known that the HA foulant layer can account for a cake layer as thick as 4 μm [35], while a skin layer thickness of RO membrane is usually less than 0.3 μm [36]. In contrast, membrane fouling by BSA used here progressed slowly and linearly until 30 h system operation, and then the slope of the permeate flux decline became steeper (Figure 5c). This trend of the permeate flux decline is again in good agreement with a previous study [31]. Permeate flux with Ludox CL dropped significantly within 5 h of system operation, then gradually decreased as filtration progressed (Figure 5d). This observation is consistent with a previous laboratory-study from which it was suggested that the hydrophobic interactions and electrostatic attraction forces between charged colloid particles and membrane surface were key causes for colloidal membrane fouling in the early filtration stage [19].

[Figure 5]

3.3. Characteristics of fouled membranes

The membrane surface hydrophobicity (measured by contact angle) increased significantly when the NF/RO membranes were fouled by tertiary effluent (Figure 6). The contact angle of the ESPA2 membrane increased from 43 to 79º due to the membrane fouling. While the three virgin membranes (NF90, ESPA2 and ESPAB) have a wide range of contact angle values (43-69º), the fouled membrane surface revealed a very similar contact angle (in the range of 66-79º). The type of foulants can also have a major impact on the hydrophobicity of membranes. The hydrophobicity of ESPA2 membranes increased as a result of membrane fouling by SA, HA and BSA, whereas a considerable reduction in hydrophobicity was observed with Ludox CL (Figure 6). The contact angle of each fouled membrane analysed here was in good agreement with results reported by Beyer et al. [33] who also investigated the hydrophobicity of fouled membranes by various model foulants using the NF270 membrane. Results reported here suggest that the hydrophobicity of the fouled membrane surface depends mainly on the hydrophobicity of the foulants.

The impact of fouling on the membrane surface charge was also examined by analysing zeta potentials of clean and fouled ESPA2 membranes. Consistent with a previous study [35], the zeta potential of the fouled membranes became less negative at high pH (i.e., pH8) and less positive at low pH (Figure 7). Amongst the model foulants, the zeta potential of BSA was similar to tertiary effluent at all pH values tested. Although organic matter eluting in tertiary effluent has a high concentration of material with similar molecular size to humic substances (Table 3), the measured zeta potential of fouled membranes by the tertiary effluent and HA were distinctly different (Figure 7). These results suggest that the material of the tertiary effluent eluting in the humic substance fraction is similar to humic acid and fulvic acid standards in terms of molecular size but has different charge characteristics. It is noted that the zeta potential analysis of the SA fouled membrane was not conducted because of the re-formation of alginate gel which clogged of the flow through cell of the Electrokinetic Analyser.

[Figure 6]

[Figure 7]

3.4. Effects of membrane fouling on inorganic salt retention

Membrane fouling by tertiary effluent led to an increase in conductivity (salt) rejection for all membranes with an exception of Ludox CL used in this investigation (Figure 8). In particular, conductivity rejection by the NF90 membrane increased significantly from 87 to 95%. Similarly, when the ESPA2 membrane was fouled by organic model foulants (SA, HA and BSA), conductivity rejection also increased. Because the fouling layer and skin layer surfaces of the RO membranes were negatively charged at pH 8 (Figure 7), the conductivity rejection increase may be attributed to an additional repelling force occurring between the fouling layer and salts. Tang et al. [32] investigated the impact of humic acid fouling using several NF/RO membranes and suggested that an increase in conductivity rejection with humic acid fouling may be attributed to an increase in repelling force between Cl^- anions and the cake layer where negatively charged humic acid is deposited (Donnan exclusion mechanism). In addition to the additional repelling force, conductivity rejection can increase when the pathways of the solute such as membrane pore (or so-called free-volume space in polymer chain [37]) and the local defects of the active skin layer are restricted with foulants. Tu et al. [38] reported a considerable increase in boron rejection when organic fouling occurred, and they suggested that the increase in boron rejection was due to the plugging of local defects or hot spots on the membrane active skin layer. In the present work, low molecular weight organic foulants present in the tertiary effluent may have narrowed down the pores within the active skin layer and/or blocked the local defects on the active skin layer surface. This additional restriction of the solute pathway may explain why the increase in conductivity rejection observed using tertiary effluent was higher than that using BSA despite their similar zeta potential of fouled membrane surface. On the other hand, the results reported here also revealed a reduction in conductivity rejection with Ludox CL fouling. Colloidal cake fouling layer depositing on membrane surface hinders back diffusion of rejected salt from the membrane surface to bulk solution, and the higher concentration gradient across the membrane is likely to result in a decrease in salt rejection (cake enhanced concentration polarisation) [31, 39]. Because the fouled membrane by colloids remarkably decreased salt rejection from 96.3% to 94.9%, the cake enhanced concentration polarisation may have played an important role in salt rejection using the fouled membrane.

[Figure 8]

3.5. Effects of membrane fouling on N-nitrosamine rejection

The rejection of small organic compounds by NF/RO membranes can be governed by steric hindrance, electrostatic interactions and adsorption onto the membrane surface [40]. All N-nitrosamines used are hydrophilic and uncharged at neutral pH, thus the electrostatic interactions and adsorption effects do not play a major role on their rejection performances. Previous studies also reported that N-nitrosamine rejection by NF/RO membranes in clean water matrices reached a steady state condition within a 45 min filtration period [3, 12]. Preliminary experimental results (Supplementary Material Figure S3) revealed no significant changes in the rejection of N-nitrosamines with the exception of NDEA after 1 and 48 h of filtration even in tertiary effluent feed. These results indicate that 1 h filtration is sufficient to evaluate the rejection of most N-nitrosamines in tertiary effluent. During the preliminary experiment, the concentration of some N-nitrosamines (i.e, NDMA, NMEA and NDBA) in the feed decreased as the filtration progressed. These N-nitrosamines have been reported to be readily biodegradable [4], and the reduction in these N-nitrosamines was possibly caused by biodegradation. A previous laboratory-scale study using the TFC-HR membrane [13] and preliminary experimental results using the ESPA2 membrane (Supplementary Material Figure S4) revealed that the effect of feed N-nitrosamine concentration on their rejections by these RO membranes is negligible in the range from 0.25 to 1.5 µg/L of each N-nitrosamine. Although the impact of N-nitrosamine concentration may vary depending on the specific membrane, the changes in N-nitrosamine feed concentration observed in this study are not expected to play an important role in the evaluation of N-nitrosamine rejections.

In general, membrane fouling by tertiary effluent caused an increase in N-nitrosamine rejection (Figure 9). This was particularly apparent for low molecular weight N-nitrosamines such as NDMA. For example, the rejection of NDMA by the NF90 and ESPA2 membranes increased in the range from 11 to 34% and from 34 to 73%, respectively. In contrast, membrane fouling on the ESPAB membrane resulted in only a slight increase (from 82 to 88%) in NDMA rejection. The results reported here also indicate that the ESPAB membrane is very effective for the removal of N-nitrosamines regardless of membrane fouling. As expected, during these filtration tests the concentrations of NDMA, NMEA and NDBA in the feed (i.e., tertiary effluent) decreased by up to 82%. The impact of SA fouling was minor, but nevertheless discernible for low molecular weight N-nitrosamines such as NDMA (Figure

10). On the other hand, membrane fouling of HA, BSA and Ludox CL had a negligible impact on the rejection of N-nitrosamines.

The clear difference in the impact of membrane fouling observed between tertiary effluent (Figure 9) and model foulants (Figure 10) is intriguing. For the separation mechanism of N-nitrosamines, the rejection of N-nitrosamines by NF/RO membranes has been reported to be mainly governed by steric hindrance where the interaction between N-nitrosamine molecule size and pore size of the active skin layer plays an important role in their rejection [13]. Because the molecular size of N-nitrosamines does not change under the experimental conditions, the increased rejection of some N-nitrosamines using the tertiary effluent is likely to be attributed to changes in membrane characteristics. It can be suggested that the pathway of solutes (such as membrane pore and local defects of the active skin layer) on RO membranes can be restricted with foulants present in the tertiary effluent (Section 3.4) or due to cake layer compression caused by the applied pressure increase, and these changes in the solute pathway leads to an increase of N-nitrosamine rejection.

[Figure 9]

[Figure 10]

4. Conclusions

Membrane fouling by tertiary effluent and organic model foulants (i.e., sodium alginate, bovine serum albumin and humic acid) led to an increase in conductivity rejection due to enhanced electrostatic interactions between the fouling layer and inorganic salts. On the other hand, colloidal fouling using Ludox CL caused a reduction in conductivity retention. Membrane fouling by tertiary effluent also increased the rejection of N-nitrosamines. The rejection of low molecular weight N-nitrosamines such as NDMA was most affected by membrane fouling and the impact was most pronounced for membranes that have high membrane permeability. Although the ESPA2 and ESPAB membranes were comparable in terms of membrane permeability and fouling susceptibility the rejection of N-nitrosamines by the ESPAB membrane was very high (over 82%) regardless the impact of membrane fouling. In contrast to the results using tertiary effluent, membrane fouling by model foulants revealed only a negligible impact on N-nitrosamine rejection. Because the tertiary effluent used in this investigation contained a high fraction of low molecular weight organic substances, these

foulants may have restricted the pathway of solutes on the active skin layer of the RO membrane, resulting in an increase in N-nitrosamine rejection. The present findings provide valuable insights for predicting NDMA rejection variations observed during full-scale RO plant operation. In addition, the results reported here indicate that changes in NDMA rejection may be predicted by analysing conductivity rejection because both rejections increased as fouling progressed. During a full-scale RO plant operation fouled membranes are generally cleaned by chemical cleaning when membrane permeability drops by 15-20%. Future work is, therefore, necessary to examine the impact of chemical cleaning on the rejection of N-nitrosamines.

5. Acknowledgements

This work was supported by the Australian Research Council Linkage Projects LP0989365 (with industry support from Veolia Water and Seqwater). The authors acknowledge the University of Wollongong for a PhD scholarship awarded to Takahiro Fujioka. The authors acknowledge Mr Kha Le Tu for his assistance with ICP-MS analysis of the tertiary treated effluent. Dow Filmtec and Hydranautics/Nitto Denko are thanked for the provision of membrane samples.

6. References

[1] A.D. Shah, W.A. Mitch, Halonitroalkanes, Halonitriles, Haloamides, and N-Nitrosamines: A Critical Review of Nitrogenous Disinfection Byproduct Formation Pathways, Environ. Sci. Technol., 46 (2011) 119-131.

[2] Y.-Y. Zhao, J. Boyd, S.E. Hrudey, X.-F. Li, Characterization of new Nitrosamines in drinking water using liquid chromatography tandem mass spectrometry, Environ. Sci. Technol., 40 (2006) 7636-7641.

[3] E. Steinle-Darling, M. Zedda, M.H. Plumlee, H.F. Ridgway, M. Reinhard, Evaluating the impacts of membrane type, coating, fouling, chemical properties and water chemistry on reverse osmosis rejection of seven nitrosoalklyamines, including NDMA, Water Res., 41 (2007) 3959-3967.

[4] J.E. Drewes, C. Hoppe, T. Jennings, Fate and transport of N-Nitrosamines under conditions simulating full-scale groundwater recharge operations, Water Environ. Res, 78 (2006) 2466-2473.

[5] USEPA, Integrated Risk Information System (IRIS), in, U.S. Environmental Protection Agency, 1993.

[6] IARC, IARC monographs on the evaluation of carcinogenic risks to humans: Overall evaluations of carcinogenicity: An updating of IARC monographs volumes 1 - 42: Supplement 7, International agency for research on cancer, (1987).

[7] NRMMC, EPHC, AHMC, Australian guidelines for water recycling: Managing health and environmental risks (Phase 2): Augmentation of drinking water supplies, Environment Protection and Heritage Council, National Health and Medical Research Council, Natural Resource Management Ministerial Council, Canberra, 2008.

[8] R. Lugg, Characterising treated wastewater for drinking purposes following reverse osmosis treatment, Premier's Collaborative Research Program, (2009).

[9] D. Sedlak, M. Kavanaugh, Removal and destruction of NDMA and NDMA precursors during wastewater treatment, in, WateReuse Foundation, Alexandria, VA, 2006.

[10] M.H. Plumlee, M. López-Mesas, A. Heidlberger, K.P. Ishida, M. Reinhard, N-nitrosodimethylamine (NDMA) removal by reverse osmosis and UV treatment and analysis via LC-MS/MS, Water Res., 42 (2008) 347-355.

[11] M.J. Farré, K. Döderer, L. Hearn, Y. Poussade, J. Keller, W. Gernjak, Understanding the operational parameters affecting NDMA formation at Advanced Water Treatment Plants, J. Hazard. Mater., 185 (2011) 1575-1581.

[12] Y. Miyashita, S.-H. Park, H. Hyung, C.-H. Huang, J.-H. Kim, Removal of N-Nitrosamines and their precursors by nanofiltration and reverse osmosis membranes, J. Environ. Eng., 135 (2009) 788-795.

[13] T. Fujioka, L.D. Nghiem, S.J. Khan, J.A. McDonald, Y. Poussade, J.E. Drewes, Effects of feed solution characteristics on the rejection of N-nitrosamines by reverse osmosis membranes, J. Membr. Sci., 409–410 (2012) 66-74.

[14] P. Xu, C. Bellona, J.E. Drewes, Fouling of nanofiltration and reverse osmosis membranes during municipal wastewater reclamation: Membrane autopsy results from pilot-scale investigations, J. Membr. Sci., 353 (2010) 111-121.

[15] R.Y. Ning, T.L. Troyer, Colloidal fouling of RO membranes following MF/UF in the reclamation of municipal wastewater, Desalination, 208 (2007) 232-237.

[16] L.D. Nghiem, S. Hawkes, Effects of membrane fouling on the nanofiltration of pharmaceutically active compounds (PhACs): Mechanisms and role of membrane pore size, Sep. Purif. Technol., 57 (2007) 176-184.

[17] A.R.D. Verliefde, E.R. Cornelissen, S.G.J. Heijman, I. Petrinic, T. Luxbacher, G.L. Amy, B. Van der Bruggen, J.C. van Dijk, Influence of membrane fouling by (pretreated) surface water on rejection of pharmaceutically active compounds (PhACs) by nanofiltration membranes, J. Membr. Sci., 330 (2009) 90-103.

475 [18] K.O. Agenson, T. Urase, Change in membrane performance due to organic fouling in
476 nanofiltration (NF)/reverse osmosis (RO) applications, Sep. Purif. Technol., 55 (2007)
477 147-156.

478 [19] K. Boussu, A. Belpaire, A. Volodin, C. Van Haesendonck, P. Van der Meeren, C.
479 Vandecasteele, B. Van der Bruggen, Influence of membrane and colloid
480 characteristics on fouling of nanofiltration membranes, J. Membr. Sci., 289 (2007)
481 220-230.

482 [20] T. Fujioka, S.J. Khan, Y. Poussade, J.E. Drewes, L.D. Nghiem, N-nitrosamine
483 removal by reverse osmosis for indirect potable water reuse – A critical review based
484 on observations from laboratory, pilot and full scale studies, Manuscript submitted to
485 Separation and Purification Technology for publication, (2012).

486 [21] R.K. Henderson, N. Subhi, A. Antony, S.J. Khan, K.R. Murphy, G.L. Leslie, V. Chen,
487 R.M. Stuetz, P. Le-Clech, Evaluation of effluent organic matter fouling in
488 ultrafiltration treatment using advanced organic characterisation techniques, J. Membr.
489 Sci., 382 (2011) 50-59.

490 [22] S.A. Huber, A. Balz, M. Abert, W. Pronk, Characterisation of aquatic humic and non-
491 humic matter with size-exclusion chromatography – organic carbon detection –
492 organic nitrogen detection (LC-OCD-OND), Water Res., 45 (2011) 879-885.

493 [23] J.A. McDonald, N.B. Harden, L.D. Nghiem, S.J. Khan, Analysis of N-nitrosamines in
494 water by isotope dilution gas chromatography-electron ionisation tandem mass
495 spectrometry, Talanta, (2012) Accepted 18 May 2012, doi:
496 2010.1016/j.talanta.2012.2005.2032.

497 [24] J.E. Drewes, C. Bellona, M. Oedekoven, P. Xu, T.-U. Kim, G. Amy, Rejection of
498 wastewater-derived micropollutants in high-pressure membrane applications leading
499 to indirect potable reuse, Environ. Prog., 24 (2005) 400-409.

500 [25] E. Van Houtte, J. Verbauwhede, Operational experience with indirect potable reuse at
501 the Flemish Coast, Desalination, 218 (2008) 198-207.

502 [26] B. Spiegelhalder, R. Preussmann, Contamination of toiletries and cosmetic products
503 with volatile and nonvolatile N-nitroso carcinogens, J. Cancer Res. Clin. Oncol., 108
504 (1984) 160-163.

505 [27] S.W. Krasner, P. Westerhoff, B. Chen, B.E. Rittmann, G. Amy, Occurrence of
506 disinfection byproducts in United States wastewater treatment plant effluents, Environ.
507 Sci. Technol., 43 (2009) 8320-8325.

508 [28] R.K. Henderson, R.M. Stuetz, S.J. Khanz, Demonstrating ultra-filtration and reverse
509 osmosis performance using size exclusion chromatography, Water Sci. Technol., 62
510 (2010) 2747-2753.

511 [29] J. Haberkamp, M. Ernst, U. Böckelmann, U. Szewzyk, M. Jekel, Complexity of
512 ultrafiltration membrane fouling caused by macromolecular dissolved organic
513 compounds in secondary effluents, Water Res., 42 (2008) 3153-3161.

514 [30] H.K. Shon, S. Vigneswaran, R.B. Aim, H.H. Ngo, I.S. Kim, J. Cho, Influence of
515 Flocculation and Adsorption as Pretreatment on the Fouling of Ultrafiltration and
516 Nanofiltration Membranes: Application with Biologically Treated Sewage Effluent,
517 Environ. Sci. Technol., 39 (2005) 3864-3871.

518 [31] L.D. Nghiem, P.J. Coleman, C. Espendiller, Mechanisms underlying the effects of
519 membrane fouling on the nanofiltration of trace organic contaminants, Desalination,
520 250 (2010) 682-687.

521 [32] C.Y. Tang, Y.-N. Kwon, J.O. Leckie, Fouling of reverse osmosis and nanofiltration
522 membranes by humic acid--Effects of solution composition and hydrodynamic
523 conditions, J. Membr. Sci., 290 (2007) 86-94.

524 [33] M. Beyer, B. Lohrengel, L.D. Nghiem, Membrane fouling and chemical cleaning in
525 water recycling applications, Desalination, 250 (2010) 977-981.

526 [34] S. Lee, W.S. Ang, M. Elimelech, Fouling of reverse osmosis membranes by
527 hydrophilic organic matter: implications for water reuse, Desalination, 187 (2006)
528 313-321.

529 [35] C.Y. Tang, Y.-N. Kwon, J.O. Leckie, Characterization of humic acid fouled reverse
530 osmosis and nanofiltration membranes by transmission electron microscopy and
531 streaming potential measurements, Environ. Sci. Technol., 41 (2006) 942-949.

532 [36] V. Freger, Swelling and morphology of the skin layer of polyamide composite
533 membranes: an atomic force microscopy study, Environ. Sci. Technol., 38 (2004)
534 3168-3175.

535 [37] Z. Chen, K. Ito, H. Yanagishita, N. Oshima, R. Suzuki, Y. Kobayashi, Correlation
536 study between free-volume holes and molecular separations of composite membranes
537 for reverse osmosis processes by means of variable-energy positron annihilation
538 techniques, The Journal of Physical Chemistry C, 115 (2011) 18055-18060.

539 [38] K.L. Tu, A.R. Chivas, L.D. Nghiem, Effects of membrane fouling and scaling on
540 boron rejection by nanofiltration and reverse osmosis membranes, Desalination, 279
541 (2011) 269-277.

542 [39] H.Y. Ng, M. Elimelech, Influence of colloidal fouling on rejection of trace organic
543 contaminants by reverse osmosis, J. Membr. Sci., 244 (2004) 215-226.

544 [40] C. Bellona, J.E. Drewes, P. Xu, G. Amy, Factors affecting the rejection of organic
545 solutes during NF/RO treatment - A literature review, Water Res., 38 (2004) 2795-
546 2809.

547

548 **Table 1**: Properties of the membranes used in this study.

Membrane	Pure water permeability[a] [L/m^{2}hbar]	Conductivity rejection[b] [%]
NF90	11.7 ± 1.1	81.2 ± 2.5
ESPA2	5.5 ± 0.3	98.1 ± 0.3
ESPAB	3.9 ± 0.2	99.3 ± 0.4

549 [a] Determined with Milli-Q water at 1,000 kPa and 20 °C feed temperature. Errors represent
550 the standard deviation of three replicates.
551 [b] Analysed with feed solution contained 20 mM NaCl, 1 mM $NaHCO_3$, 1 mM $CaCl_2$ at
552 permeate flux 20 L/m^{2}h, cross flow velocity 40.2 cm/s, feed pH 8.0 ± 0.1 and feed
553 temperature 20.0 ± 0.1 °C.

554 **Table 2:** Water quality of the tertiary effluent.

Parameter	Value
Turbidity	0.7 NTU
Conductivity	790 µS/cm
pH	7.8
TOC	9.3 mg/L
Na^+	106 mg/L
Mg^{2+}	14 mg/L
K^+	17 mg/L
Ca^{2+}	23 mg/L
Fe^{2+}	13 mg/L
Cl^-	177 mg/L
NO_3^-	43 mg/L
SO_4^{2-}	46 mg/L

555

556 **Table 3:** Organic matter fractions in each feed solution.

	Tertiary effluent	BSA	Sodium alginate	Humic acid
Hydrophobic [%]	11.1	n.q.	2.0	0.4
Hydrophilic				
Biopolymer [%]	9.8	79.5	91.1	5.6
Humics [%]	50.8	n.q.	n.q.	68.4
(Mean MW [g/mol])	(467)			(850)
Building blocks [%]	15.1	8.1	2.2	9.2
LMW neutrals [%]	12.6	22.4	2.6	16.4
LMW acid [%]	0.6	0.2	2.1	n.q.

557 *n.q., not quantifiable

Effects of membrane fouling on N-nitrosamine rejection by nanofiltration and reverse osmosis membranes

Journal of Membrane Science

Takahiro Fujioka [1], Stuart J. Khan [2], James A. McDonald [2], Rita K. Henderson [2], Yvan Poussade [3,4], Jörg E. Drewes [2, 5], and Long D. Nghiem [1,*]

[1] Strategic Water Infrastructure Laboratory, School of Civil Mining and Environmental Engineering, The University of Wollongong, NSW 2522, Australia

[2] UNSW Water Research Centre, School of Civil and Environmental Engineering, The University of New South Wales, NSW 2052, Australia

[3] Veolia Water Australia, Level 15, 127 Creek Street, QLD 4000, Australia

[4] Seqwater, Level 2, 240 Margaret St, Brisbane City QLD 4000 Australia

[5] Advanced Water Technology Center (AQWATEC), Department of Civil and Environmental Engineering, Colorado School of Mines, Golden, CO 80401, USA

SUPPLEMENTARY MATERIAL

* Corresponding author: Long Duc Nghiem, Email: longn@uow.edu.au, Ph +61 2 4221 4590

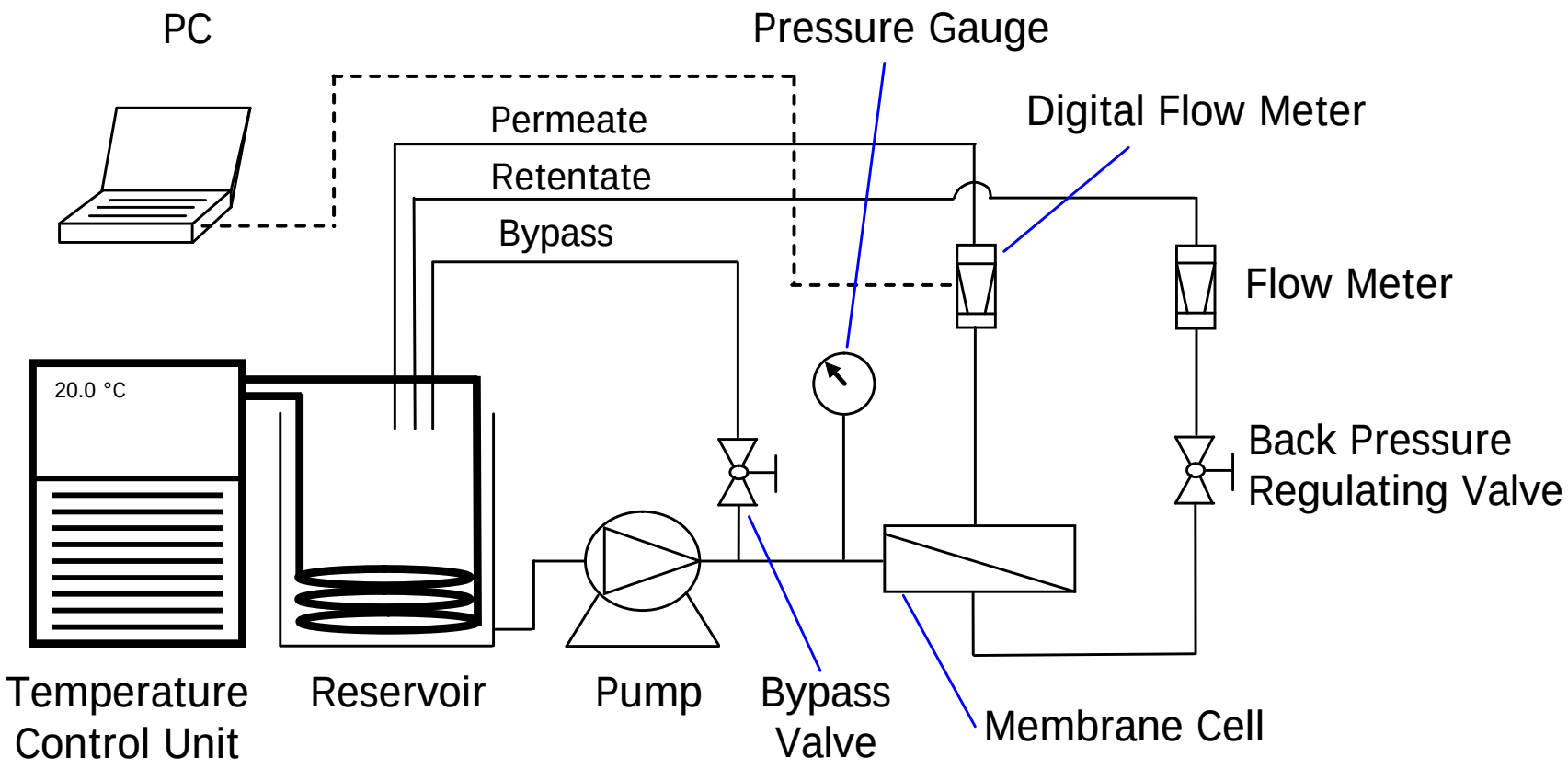

Figure S1: Schematic diagram of the cross flow filtration system.

Table S2: Membrane permeability by the clean and fouled membranes.

Membrane	Feed solution		Clean [$Lm^{-2}h^{-1}bar^{-1}$ at 20°C]	Fouled [$Lm^{-2}h^{-1}bar^{-1}$ at 20°C]
NF90	Tertiary effluent		11.1	5.7
ESPAB	Tertiary effluent		3.3	2.7
ESPA2	Tertiary effluent	1st	4.9	3.6
		2nd	5.0	3.5
	Sodium alginate	1st	4.5	2.6
		2nd	4.6	3.0
	Humic acid	1st	5.0	2.9
		2nd	5.0	3.6
	BSA	1st	4.7	4.0
		2nd	4.7	3.7
	Ludox CL	1st	4.9	3.5
		2nd	4.7	3.3

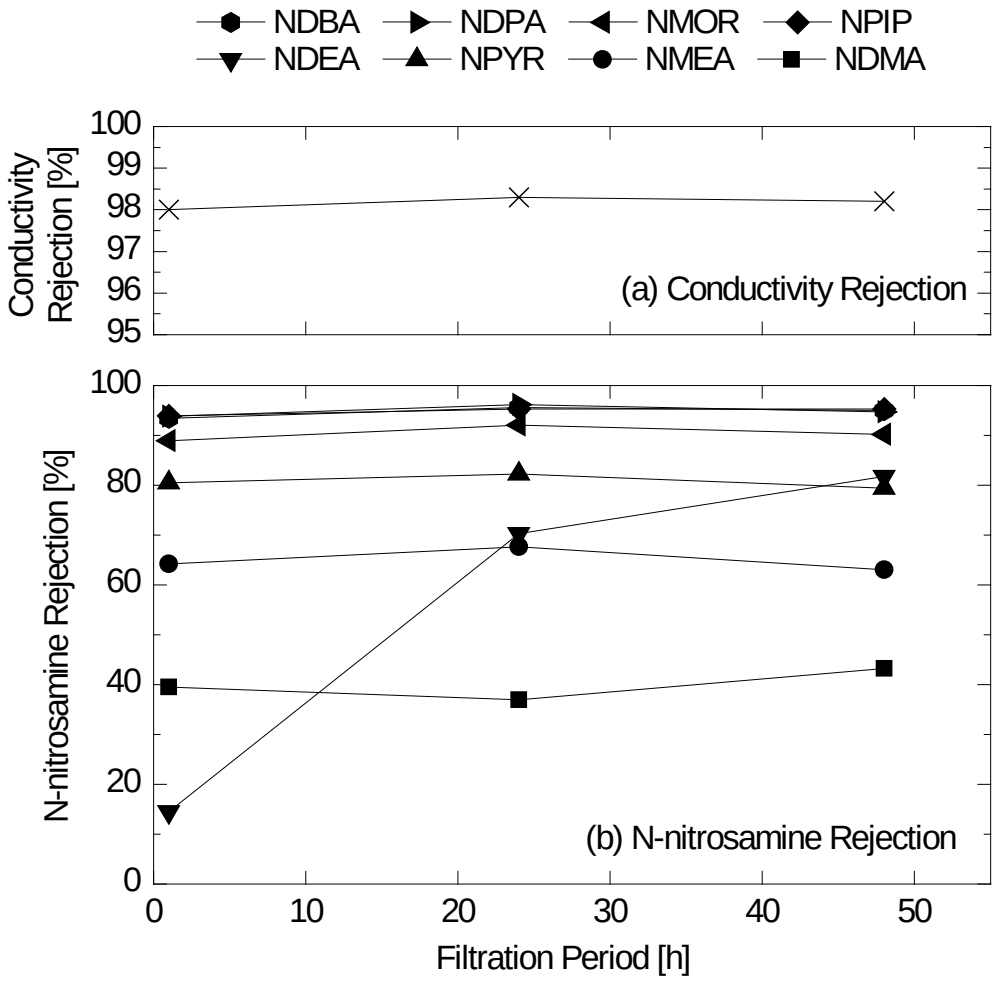

Figure S3: (a) Conductivity rejection and (b) N-nitrosamine rejection by the ESPA2 membrane as a function of filtration period (permeate flux 20 L/m^{2}h, crossflow velocity 40.2 cm/s, feed temperature 20.0 ± 0.1 °C).

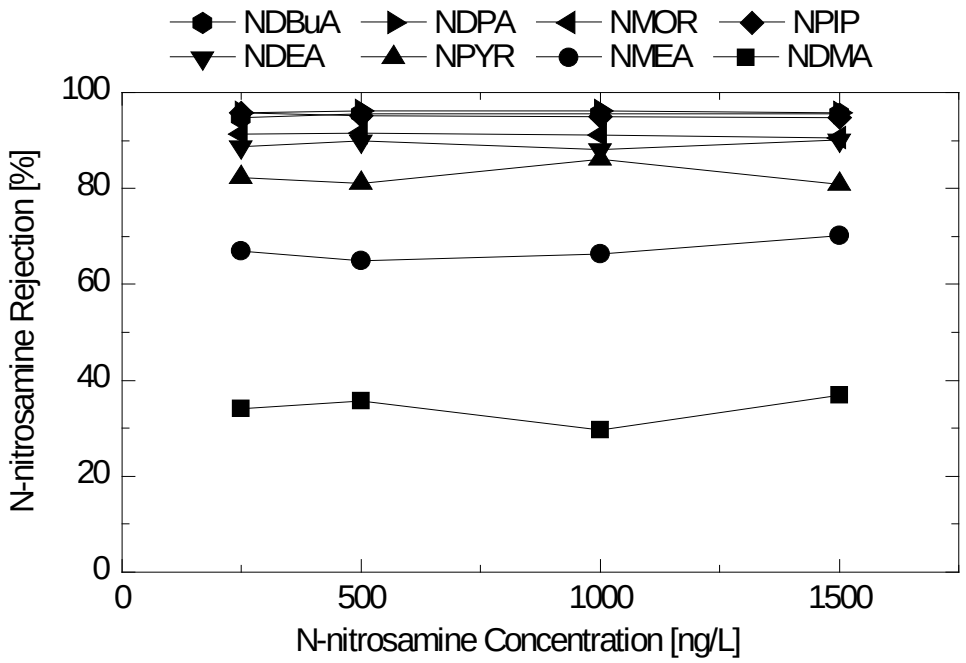

Figure S4: Rejection of N-nitrosamines by ESPA2 membrane as a function of nitrosamine concentration in the feed (20 mM NaCl, 1 mM $NaHCO_3$, 1 mM $CaCl_2$, permeate flux 20 L/m^2h, crossflow velocity 40.2 cm/s, feed pH 8.0±0.1, feed temperature 20.0±0.1 °C).